Integrated Position and Speed Loops Under Sliding-Mode Control Optimized by Differential Evolution Algorithm for PMSM Drives

Zhonggang Yin, *Member, IEEE*, Lei Gong, Chao Du, *Student Member, IEEE*, Jing Liu, and Yanru Zhong

***Abstract*—In this paper, to improve the robustness and realize the precision positioning as well as speed control of the servo drive system, an integrated sliding-mode control (ISMC) optimized by differential evolution (DE-ISMC) algorithm is proposed. ISMC guarantees that a motor can reach at given position with given speed, and given speed is set first. ISMC, which is combined with speed regulator and position regulator, is different from the conventional sliding-mode control (SMC) replacing speed regulator. ISMC can guarantee that motor speed is controlled under position control mode, which is a novelty and an advantage of ISMC in this paper. To achieve good control performance of ISMC, parameters of it should be chosen exactly, so DE algorithm is selected to optimize them. The most significant influence factor of DE algorithm is the optimization iteration. Once parameters of ISMC are optimized under convergent iteration, servo system performance reaches given indices in the shortest time. Experimental results indicate that robustness of the servo system is improved; correctness and effectiveness of DE-ISMC are verified.**

***Index Terms*—Differential evolution (DE) algorithm, integrated sliding-mode control (ISMC), iteration, parameters optimization, servo drive system.**

I. Introduction

SERVO motors can be controlled similarly as DC motors using the field-oriented control (FOC) approach, and performance of servo motor with FOC is comparable to those of DC motors. As modern industrialization and permanent magnet material develop, AC servo drive systems with permanent magnet synchronous motor (PMSM) are used widely in many areas. However, the servo motor drive still has a series of challenging problems due to some causes including parameter variation, model mismatch, load disturbance, and nonlinear nature. These issues are devoted to deteriorating performance such as

Manuscript received March 14, 2018; revised July 30, 2018 and November 6, 2018; accepted December 10, 2018. Date of publication January 1, 2019; date of current version June 10, 2019. This work was supported in part by the National Natural Science Foundation of China under Grant 51677150, in part by the Specialized Research Fund of Shaan Xi Province under Grant 2015KJXX-29, and in part by the State Key Laboratory of Large Electric Drive System and Equipment Technology under Grant SKLLDJ012016006. Recommended for publication by Associate Editor G. Escobar. *(Corresponding author: Zhonggang Yin.)*

The authors are with the Xi'an University of Technology, Xi'an 710048, China (e-mail:

speed loop or individual position loop of servo control system. Therefore, integrated sliding-mode control (ISMC) can guarantee that motor speed is controlled under position control mode. In some special situations, motor rotor needs to arrive at a given position with a given speed. In order to solve this problem, the position loop based on SMC and the speed loop based on SMC need to be merged; hence, the ISMC is proposed to replace position and speed loops. In order to guarantee that motor rotor can reach at the given position with the given speed, a specified speed profile must be devised in advance. It is usual to design a trapezoidal speed profile obtaining three segments, which are acceleration segment, constant speed segment (run segment), and deceleration segment. Different control structures are designed in different segments. In consideration of a structure of the controller, ISMC is a better choice to be applied in the servo drive system. ISMC simplifies conventional structures of servo drive systems, and a servo drive system only contains two controllers, which are ISMC and current regulator.

Due to the requirement of the precise positioning with the given speed in industrial applications, it has a direct and significant impact on the servo system response performance. Suitable reaching law of ISMC is also important, as well as parameters of reaching law need to be chosen properly. Therefore, tuning parameters is a significant step in the system design. Generally, designer of ISMC adopts a trial-and-error tune method. However, processes of manually tuning ISMC parameters are time consuming and require a mass of design efforts, and it is difficult to satisfy given performance indices in finite time. If parameters are not tuned properly, performance of ISMC will be affected, and then it will limit wide applications of ISMC method. Consequently, it is essential to look for a method to tune parameters of ISMC in the servo drive system.

In order to control motor speed during positioning, the ISMC based on DE algorithm is proposed in this paper. ISMC is not a simple and conventional controller; the speed signal could be controlled indirectly in conventional SMC and directly in the ISMC. In other words, the motor speed in the ISMC is seen as a given signal instead of a measured signal. The ISMC, which is combined with speed regulator and position regulator, is different from the conventional SMC. DE is known for its simplicity, robustness, and rapid performance. Compared with most intelligence algorithms (genetic algorithms, particle swarm optimization), the DE algorithm has less calculation to realize optimization processes. The less calculation leads to the rapid dynamic performance, which is a key index in the servo drive system. In [19], it presents a modified JADE version with sorting crossover rate (CR). In the proposed algorithm, a smaller CR value is assigned to the individual with better fitness value. Therefore, the components of the individuals, which have better fitness values, can appear in the offspring with higher possibility. In addition, the better offsprings generated from last iteration are supposed to have better schemes. In [20], the technology electrical continuously variable transmission (E-CVT) system provides the opportunity to fulfill this requirement. However, conventional E-CVT with planetary gears suffers from frictional loss, high maintenance, and audible noise. The paper adopted a differential evolution algorithm coupled with finite element method to optimize torque, energy efficiency, torque ripples, and multiobjective of the E-CVT system by reconfiguring the height of rotors, the areas of slots, and the height of yoke. In order to balance the conflicting goals of fuel consumption and emissions reduction in the choice of operating point, the adaptive multiobjective differential evolution algorithm is proposed to solve the auxiliary power unit operating point multiobjective optimization problem in [21]. There are many control parameters in the ISMC, thus, the DE algorithm is used to optimize them, and make control performance achieve the given indices. Moreover, DE algorithm has good robustness, so it is more appropriate to be combined with ISMC. The similar control structures of ISMC model had been proposed in [22], but the design principle of SMC is totally different between the work done in [22] and this paper. DE algorithm has been used previously in some other fields such as neural network, pattern recognition, and power system, and shown its superiority in the aforementioned fields. However, the DE algorithm has been rarely applied in the servo drive system previously; therefore the controller is simplified and its parameters are optimized by the DE algorithm in this paper, and the servo system achieves the given performance indices. It can make ISMC have better control performance such as less chattering and better dynamic performance by combining it with the DE algorithm.

Based on above mentioned analyses, a novel integrated control method of servo drive for position and speed loops based on SMC with differential evolution algorithm is proposed. In order to optimize parameters of ISMC, the DE algorithm is adopted. The advantages of ISMC and DE algorithm are combined, and the DE algorithm is used to optimize the parameters of ISMC with suitable iteration. DE-ISMC improves the robustness of the servo drive system and achieves the given control indices when the motor parameters mismatch and load disturbance. At the same time, the low speed crawling phenomenon of servo drive system is relieved and achieves given indices after convergent iteration. The correctness and effectiveness of the proposed method are verified by experimental results.

II. Mathematical Model of Servo Drive System

The type of servo motor used is PMSM, assuming that a servo motor is an ideal controlled object, and a mathematical model of a servo motor under the *d-q* coordinate system is given as follows:

$$\begin{cases} u_d = Ri_d - \omega L_q i_q + L_d \frac{di_d}{dt} \\ u_q = Ri_q + \omega L_d i_d + \omega \psi_f + L_q \frac{di_q}{dt} \end{cases} \tag{1}$$

$$T_e = 1.5 n_p (\psi_f i_q + (L_d - L_q) \cdot i_d \cdot i_q). \tag{2}$$

The servo motor motion formula is

$$T_e - T_L = \frac{J}{n_p} \frac{d\omega}{dt} \tag{3}$$

where u_d and u_q represent *d*-axis stator voltage and *q*-axis stator voltage, respectively. i_d and i_q are *d*-axis current and *q*-axis current, respectively. L_d and L_q represent *d*-axis stator inductance and *q*-axis stator inductance, respectively. R_s is stator resistance, ψ_f is flux linkage of permanent magnets, ω is electrical

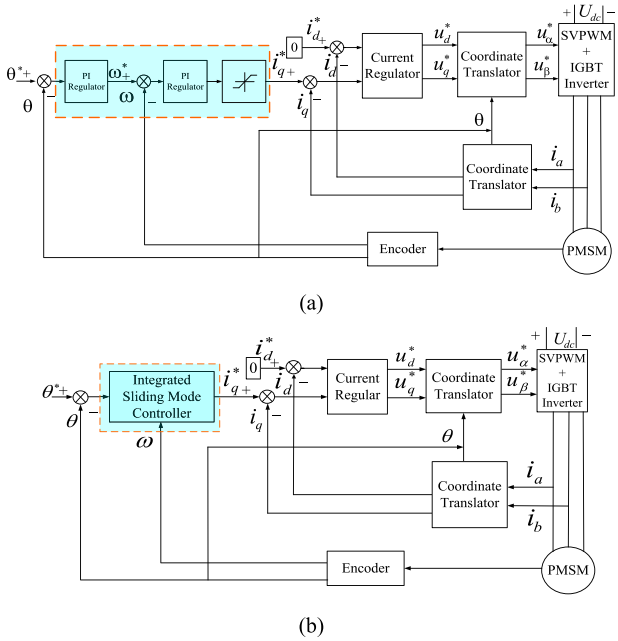

Fig. 1. Block diagram of servo system based on field-oriented: (a) conventional PI controller and (b) ISMC.

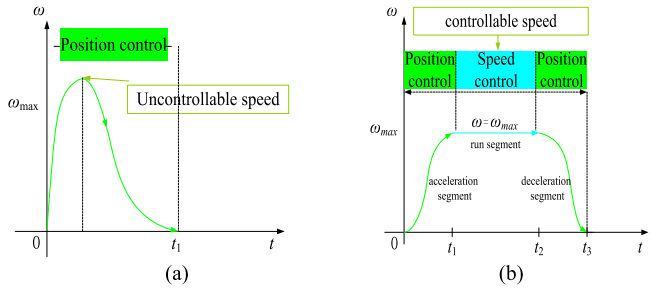

Fig. 2. Simplified speed profile of servo drive system based on field-oriented: (a) conventional SMC and (b) ISMC.

angular velocity, J is rotational inertia, T_e is electrical magnetic torque, T_L is load torque, and n_p is number of pole pairs.

The block diagram of simplified servo system based on field-oriented approach is shown in Fig. 1. Generally, conventional regulators are replaced by PI controllers which are shown in Fig. 1(a). In some cases, such as parameters mismatch, low speed crawling, and load disturbance, a position or speed regulator is replaced individually by single sliding mode controller to improve the servo system robustness. The proposed ISMC that integrates position and speed loops is shown in Fig. 1(b). The proposed SMC not only simplifies the system structure, but also improves system robustness effectively. Besides, it can simultaneously achieve control of both speed and position of a motor rotor.

III. Integrated Control Based on SMC of Servo Motor

SMC is a kind of special non-linear control method, and it is convenient to be realized physically. Thus, SMC is applied widely to adapt to different control requirements. Then, PI regulators are often replaced by SMC because motor speed cannot be controlled in traditional SMC methods under position control mode as shown in Fig. 2(a), and the extreme armature current is produced if motor speed is too large. In order to guarantee the motor security working against over current conditions, the ISMC is proposed. This method contains two kinds of control modes, including speed control and position control. In Fig. 2(b), a trapezoidal speed profile has three parts under position and speed control modes: acceleration segment s_1 (under position control mode), run segment s_2 (under speed control mode), and deceleration segment s_3 (under position control mode).

In terms to different segments of servo motor motion, different sliding mode surfaces are needed to get in advance. In order to achieve positioning control, both rotor speed and rotor position need to be controlled at the same time. In Fig. 2(b), when motor speed arrives at $\omega_{\max}$ at t_1, the control mode is switched to speed control mode, which maintains motor rotor speed at $\omega_{\max}$, instead of exceeding $\omega_{\max}$ and decelerating fast, as shown in Fig. 2(a). At t_2, actual motor rotor position is close to reference position, and the sliding control mode is switched to position control mode immediately. In order to keep trapezoidal profile symmetric, t_2 can be calculated. For example, first, when motor runs at t_1, the route is 20% of the whole given position signal, then when motor runs 80% of the whole given position signal, motor speed is ready to slow down, and t_2 is calculated. Afterward, motor rotor stops at t_3. When the given position signal is of few degrees, speed profile transforms from trapezoidal shape into triangular shape. In this case, the rotor could achieve given position in few seconds, and motor speed has few effects on the control performance. The principle and basic design of ISMC in the servo system are introduced as follows.

A. Position Control Mode

Assuming state variables are designed as follows:

$$\begin{cases} x_1 = \theta^* - \theta \\ x_2 = \dot{x}_1 = -\omega. \end{cases} \tag{4}$$

Combining (3) and (4), we obtain

$$\dot{x}_2 = -\dot{\omega} = -\frac{n_p}{J}(T_e - T_L). \tag{5}$$

The following formula is reached by substituting (2) into (5), taking into account that $i_d^* = 0$ (see Fig. 1):

$$\dot{x}_2 = -\frac{n_p}{J}(1.5 n_p \psi_f i_q - T_L). \tag{6}$$

Once again, when the servo motor is operation with no load, i_q^* is near 0. The torque current which is shown in the experiment is near 0, and $T_L = 0$, $\dot{x}_2$ is expressed as

$$\dot{x}_2 \approx -\frac{n_p}{J}(1.5 n_p \psi_f i_q) = -A i_q \tag{7}$$

where $A = 1.5\frac{{n_p}^2}{J}\psi_f$.

During the time of [0, t_1] and [t_2, t_3] in Fig. 2(b), both the acceleration segment s_1 and the deceleration segment s_3 are under position control mode. Either motor rotor speed arrives at $\omega_{\max}$ with forward acceleration or actual rotor position is close

to the reference position, then a relative sliding mode surface is designed as

$$s_{1,3} = k_1 x_1 + x_2 \tag{8}$$

where k_1 is a positive constant. In order to ensure that motor rotor speed arrives at $\omega_{\max}$ and reduces chattering more quickly, the exponential reaching law is given as

$$\dot{s}_{1,3} = -\varepsilon_1 \mathrm{sgn}(s_{1,3}) - c_1 s_{1,3} \tag{9}$$

where $\varepsilon_1 > 0, c_1 > 0$. ε_1 and c_1 are switching gain and exponent coefficients of the reaching law, respectively. When a servo drive system is stable, (9) can be developed as

$$-\varepsilon_1 \mathrm{sgn}(s_{1,3}) - c_1 s_{1,3} = k_1 \dot{x}_1 + \dot{x}_2. \tag{10}$$

Combining (7) and (10), we get

$$i_{q1,3} = \frac{1}{A} \cdot [\varepsilon_1 \mathrm{sgn}(s_{1,3}) + c_1 s_{1,3} - k_1 \omega]. \tag{11}$$

Based on results of aforementioned analyses, k_1, ε_1, and c_1 have a vital impact on control performance of s_1 and s_3. However, it is inconvenient to select appropriate k_1, ε_1, and c_1 to improve the robustness when servo motors suffer from disturbance. Hence, it is necessary to find an efficient way to optimize appropriate parameters.

B. Speed Control Mode

During the time of $[t_1, t_2]$ in Fig. 2(b), the servo motor rotor speed is $\omega_{\max}$. In order to make a good control performance under speed control mode, $\omega_{\max}$ is needed to design a variable value. According to different reference positions, when reference position is small, $\omega_{\max}$ is small accordingly. Similarly, when reference position is large, the $\omega_{\max}$ is large accordingly. In other words, in order to ensure that motor fix position quickly, $\omega_{\max}$ should be set as a larger value when reference position is larger.

The sliding mode surface of run segment s_2 is designed as

$$s_2 = x_2 + \omega_{\max}. \tag{12}$$

Equation (12) can be described as

$$s_2 = (\theta^* - \theta)' + \omega_{\max}. \tag{13}$$

It is more convenient to design SMC with (13), and once servo drive system runs on $s_2 = \omega_{\max}$, the motor rotor speed is $\omega_{\max}$. Similar to (9), the exponential reaching law of $\dot{s}_2$ is given as

$$\dot{s}_2 = -\varepsilon_2 \mathrm{sgn}(s_2) - c_2 s_2 \tag{14}$$

where $\varepsilon_2 > 0, c_2 > 0$. ε_2 and c_2 are switching gain and exponent coefficients of the reaching law, respectively. When the servo drive system is stable (14) can be developed as

$$-\varepsilon_2 \mathrm{sgn}(s_2) - c_2 s_2 = -A \cdot i_{q2}.$$

Combining (13) and (14), the sliding mode speed controller is obtained as

$$i_{q2} = \frac{1}{A} \cdot [\varepsilon_2 \mathrm{sgn}(s_2) + c_2 s_2]. \tag{15}$$

According to (15), ε_2 and c_2 have an important impact on run segment s_2. However, it is inconvenient to select appropriate ε_2 and c_2 to improve robustness when a servo motor suffers from disturbance.

i_q output expression is under postion mode and speed mode, respectively. The i_q limitation of ISMC is set in the limiter to avoid shock current. When servo motor is operation with full load or 10% full load, T_L is a constant. In order to embody strong robustness of the servo system, the concrete value of i_q is not calculated, and the more suitable parameters of ISMC is optimized in due course. Experimental results indicate that robustness of the servo system is improved, and correctness and effectiveness of DE-ISMC are verified when T_L is not zero.

C. Stability Analysis of ISMC

The stability analyses of the acceleration segment s_1 and the deceleration segment s_3 are shown as follows.

According to the Lyapunov stability theory, if $\dot{V}(x) = s \cdot \dot{s} \leq 0$ exists, the servo drive system is stable. The Lyapunov function is

$$V(x) = \frac{1}{2} s^2. \tag{16}$$

From (8), (9), and (16), we obtain (17) as

$$\begin{aligned} \dot{V}(x) &= s_{1,3} \cdot \dot{s}_{1,3} = (k_1 x_1 + x_2) \cdot (-\varepsilon_1 \mathrm{sgn}(s_{1,3}) - c_1 s_{1,3}) \\ &= -(k_1 x_1 + x_2) \cdot [\varepsilon_1 \mathrm{sgn}(k_1 x_1 + x_2) + c_1 (k_1 x_1 + x_2)] \\ &= -\varepsilon_1 (k_1 x_1 + x_2) \cdot \mathrm{sgn}(k_1 x_1 + x_2) - c_1 (k_1 x_1 + x_2)^2 \\ &= -\varepsilon_1 \cdot |k_1 x_1 + x_2| - c_1 (k_1 x_1 + x_2)^2 \leq 0. \end{aligned} \tag{17}$$

Similarly, (12), (14), and (16) are combined, and the stability analysis of the run segment s_2 is verified as follows:

$$\begin{aligned} \dot{V}(x) &= s_2 \cdot \dot{s}_2 = (x_2 + \omega_{\max}) \cdot (-\varepsilon_2 \mathrm{sgn}(s_2) - c_2 s_2) \\ &= -(x_2 + \omega_{\max}) \cdot [\varepsilon_2 \mathrm{sgn}(x_2 + \omega_{\max}) + c_2 (x_2 + \omega_{\max})] \\ &= -\varepsilon_2 (x_2 + \omega_{\max}) \cdot \mathrm{sgn}(x_2 + \omega_{\max}) - c_2 (x_2 + \omega_{\max})^2 \\ &= -\varepsilon_2 \cdot |x_2 + \omega_{\max}| - c_2 (x_2 + \omega_{\max})^2 \leq 0. \end{aligned} \tag{18}$$

According to (17) and (18), the stability of the ISMC is verified.

IV. Optimized ISMC Using Differential Evolution Algorithm

If robustness of servo drive systems needs to be improved effectively, main ISMC parameters k_1, ε_1, c_1, ε_2, and c_2 of three segments must be appropriate. However, it is rather hard to choose the most suitable controller parameter to achieve the given performance indices by tuning them manually. Consequently, in this paper, the differential evolution algorithm is introduced to optimize these parameters. After making use of parameters optimized by the DE, robustness of the servo systems is strengthened, and the dynamic and steady performance is optimized simultaneously. A novel DE-ISMC method is proposed in this section, and it employs that DE algorithm can tune parameters of ISMC automatically. Moreover, experimental

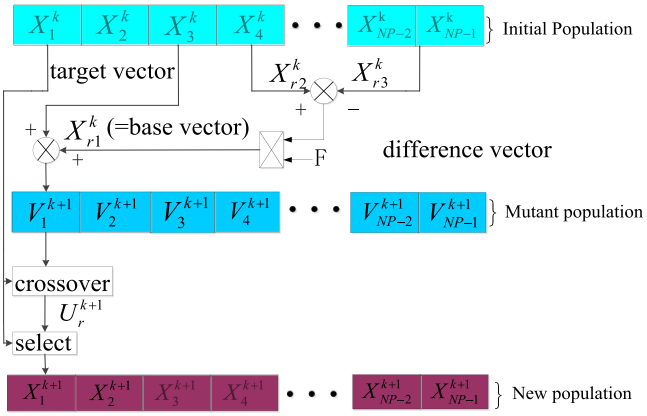

Fig. 3. Main processes of the DE algorithm.

results verify that DE-ISMC is more likely to make the dynamic and steady performance better than ordinary ISMC.

A. Processes of DE Algorithm

The same as other principles of evolutionary algorithms, DE algorithm is also a kind of multi-point search algorithm. Some optimization processes of DE algorithm are similar to that of genetic algorithm. Main processes of DE algorithm are shown in Fig. 3. Main objective of DE algorithm is that, DE algorithm selects two random vectors, which are from initialization populations, and then it creates mutated generation by factor F and another random vector. Next, a new generation is evolved and generated after crossover and selection. Concrete processes are illustrated as follows.

1) Initialization: Like other evolutionary algorithms, at the beginning of optimization, DE algorithm also needs initial populations, and the population size is identified as N_P. The random initial population is from a known range value covering whole parameters space.

Setting $X_i = [x_{i1}, x_{i2}, \ldots, x_{\mathrm{in}}]$, where n means solution space dimension, and an individual vector $X_{i,j}$ is emerged by (19)

$$x_{i,j} = x_{i,j\,\min} + r\ \text{and}(0,1) * (x_{i,j\,\max} - x_{i,j\,\min}) \tag{19}$$

where $x_{i,j}$, $x_{i,j\,\max}$, and $x_{i,j\,\min}$ are jth components, upper limit, and lower limit of an individual vector X_i, respectively.

2) Mutation: According to the K generation vector X_i^k, then mutated vector $v_{i,j}^{k+1}$ is produced by

$$v_{i,j}^{k+1} = x_{r1,j}^k + F \cdot (x_{r2,j}^k - x_{r3,j}^k) \tag{20}$$

where $x_{r1,j}^k, x_{r2,j}^k$, and $x_{r3,j}^k$ are jth components of three different and random vectors from the K generation individuals. Factor F is a significant parameter to control differential quantity.

3) Crossover: Crossover factor is presented to improve interference vector diversity in the DE algorithm, target vector $u_{i,j}^{k+1}$ is engendered from mutation and source vectors, and each variable is calculated as

$$u_{i,j}^{k+1} = \begin{cases} v_{i,j}^{k+1} & \eta_j \le \mathrm{C}_R \text{ or } j = q_j \\ x_{i,j}^k & \text{otherwise} \end{cases} \tag{21}$$

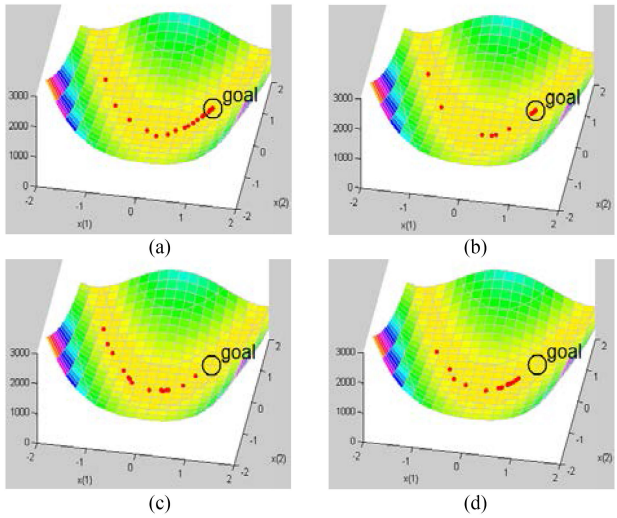

Fig. 4. Main parameters influence of the DE algorithm. (a) F = 0.5, C_R = 0.9, N_P = 100, iteration = 20. (b) F = 0.8, C_R = 0.9, N_P = 100, iteration = 20. (c) F = 0.5, C_R = 0.5, N_P = 100, iteration = 20. (d) F = 0.5, C_R = 0.9, N_P = 100, iteration = 15.

where q_j is a random integer that belongs to (1, n), $\eta_j \in (0, 1)$ is a random control parameter of the j-dimensional component. The crossover factor $C_R \in (0, 1)$ controls the diversity of the populations, as well as helps algorithm escape from local optimal solution.

4) Selection: By principle of the greedy selection, once the individual evolution value is better, the better individual is reserved as the new group. If not, the parent individuals are still remained in the populations, and this section is described as

$$x_{i,j}^{k+1} = \begin{cases} u_{i,j}^{k+1} & \text{if} \quad f(u_{i,j}^{k+1}) < f(x_{i,j}^k) \\ x_{i,j}^k & \text{otherwise.} \end{cases} \tag{22}$$

All processes of the DE algorithm are shown earlier, and Fig. 4 shows the influence of parameters F, C_R, and iteration. In Fig. 4, red dots represent individuals, black circle represents optimization goal. Population quantity N_P is chosen from 50 to 200. The range of F and C_R is (0, 2) and (0, 1) in the evolution, respectively. Mutation factor F decides the ratio of deviation vector, Fig. 4(a) and (b) displays that convergence rate is faster when F is 0.5 instead of 0.8, which means that smaller mutation factor F is, the faster convergence rate is. Comparing results of Fig. 4(a) and (c), the larger the crossover factor C_R is, the faster the convergence rate is. Comparing results of Fig. 4(a) and (d), it is evident that more iterations are more likely to improve convergence rate of DE algorithm. On the contrary, more iterations cost much time, thus suitable iteration is chosen from 5 to 50. Finally, chosen parameters of DE algorithm are $N_P = 100$, $F = 0.5$, $C_R = 0.9$ in the proposed DE-ISMC, and concrete iteration depends on running conditions of servo drive systems.

B. ISMC Based on DE Algorithm for the Servo Drive System

In order to study DE-ISMC method for servo drive systems, the block diagram of DE-ISMC based on FOC is shown in Fig. 5.

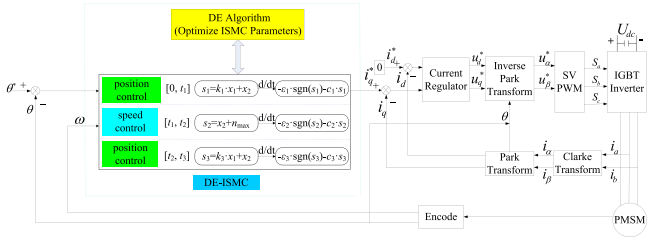

Fig. 5. Block diagram of the servo drive system based on DE-ISMC method.

DE-ISMC method mainly comprises two parts to optimize ISMC parameters based on DE algorithm; these two parts are parameters optimization by DE algorithm and ISMC. According to analyses given in Section III, it is known that the control performance of ISMC is greatly affected by k_1, ε_1, c_1, ($k_1 = k_3$, $\varepsilon_1 = \varepsilon_3$, $c_1 = c_3$), ε_2, and c_2. Thus, these five variables need to be optimized to achieve given performance indices.

In Fig. 5, θ^* and θ represent reference position and actual position, respectively. ω is electrical angular velocity. i_q^* and i_q represent reference q-axis current and actual q-axis current, respectively. i_α and i_β represent α-axis current and β-axis stator current, respectively. i_a and i_b represent a-phase current and b-phase current, respectively. S_a, S_b, and S_c represent switching vectors.

When servo motor is operation with no load, i_q^* is near 0. The torque current which is shown in the experiment is near 0, although the three SMC algorithms are switched. When the servo motor is added with rated load suddenly, the torque is varied from 0 to rated value, as shown in Figs. 22 and 23. It means that i_q^* varies from 0 to a concrete value. According to $T_e = 1.5 n_p \psi_f i_q$, the concrete i_q^* value can be achieved. ω in (11) and Fig. 5, is the motor speed, which can be obtained from feedback signals of encoder. In (4), x_1 and x_2 both contain ω, and $k_1\omega$ is taken into account as a part of x_1 and x_2.

In order to improve control performance of servo drive systems, DE algorithm is applied to optimize the above mentioned five parameters. Next, concrete processes of adapting DE algorithm are illustrated as follows.

1) Establishment of the Objective Function: To achieve better control performance and robustness of servo systems, five key parameters of ISMC are optimized by the DE algorithm. Therefore, an objective function that reflects performance of systems is designed to satisfy control indices set.

Ordinarily, the performance of the servo drive system includes dynamic performance and steady performance. Dynamic performance mainly includes speed rise time T_{rise}, motor loading recovery time T_{rerl}, unloading recovery time T_{renl}, motor loading speed drop percentage ΔN_{ovdrop} (%), and motor unloading speed up percentage ΔN_{ovup} (%). Steady performance is speed steady error percentage $E_{\text{ss\_spe}}$ (%). The corresponding indices of relative performance are defined as $T_{\text{rise-index}}$, $\Delta N_{\text{ovdrop-index}}$, $\Delta N_{\text{ovup-index}}$, $T_{\text{rerl-index}}$, $T_{\text{renl-index}}$, and $E_{\text{ss\_spe-index}}$, respectively. n and $n_{\max}$ is the actual speed and given maximum speed of the motor, respectively, and $n_{\max}$ is relative to the reference position. Concrete performance indices can be set based on the given performance indices, and the optimization iteration and controller parameters are varied as different given performance indices. In order to make the objective function achieve control indices with different cases including parameter mismatch, low speed crawling, and load disturbance, it is composed of weighted sum of dynamic and steady given performance indices.

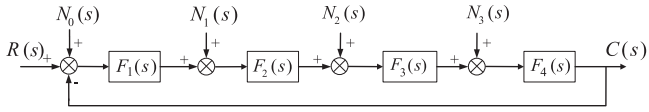

Fig. 6. Block diagram of the servo drive system.

When a servo system is under parameter mismatch or low speed crawling, the objective function is shown as

$$Y = \begin{cases} Y_{1,3} = |k_1 \cdot (T_{\text{rise}} - T_{\text{rise-index}}) \\ \qquad + (\varepsilon_1 + {c_1}^2) \cdot (n - n_{\max})| \quad [0, t_1] \text{ or } [t_2, t_3] \\ Y_2 = |\varepsilon_2 \cdot (n - n_{\max}) + c_2 \\ \qquad \cdot (E_{\text{ss\_spe}} - E_{\text{ss\_spe-index}})| \quad [t_1, t_2]. \end{cases} \tag{23}$$

Once the system experiences load disturbance, Y_2 is switched as

$$\begin{aligned} Y_2 = |\varepsilon_2 \cdot (&\Delta N_{\text{ovdrop}} + \Delta N_{\text{ovup}} + n - \Delta N_{\text{ovdrop-index}} \\ &- \Delta N_{\text{ovup-index}} - n_{\max}) + c_2 \cdot (T_{\text{rerl}} + T_{\text{renl}} + E_{\text{ss\_spe}} \\ &- T_{\text{rerl-index}} - T_{\text{renl-index}} - E_{\text{ss\_spe-index}})| \end{aligned}$$

where $\omega_{\max}$ is changed as $n_{\max}$. Unit of $\omega_{\max}$ is rad/s, unit of $n_{\max}$ is r/min, and $\omega_{\max}$ and $n_{\max}$ have an equation: 1 r/min = 2π/60 rad/s. The objective function of a system is determined by the aforementioned design. In other words, the smaller Y is, the better performance of a system is. Thus, given performance indices can be achieved until Y reaches the minimum value.

2) Parameter Optimization of ISMC: Fig. 6 shows the block diagram of a servo drive system. $R(s)$ is input and $N_0(s)$ is input interference. $F_1(s)$, $F_2(s)$, $F_3(s)$, and $F_4(s)$ are transfer functions of different levels, respectively. $C(s)$ is output and $E(s)$ is error. $N_1(s)$, $N_2(s)$, and $N_3(s)$ are disturbance of each level, respectively.

The servo motor model can be seen as an inertial element. The conventional servo drive system contains three loops, which are current loop, speed loop, and position loop. According to the mathematical model of motor structure, the servo motor model and the design of each loop are shown as follows.

Design of the servo motor model $F_4(s)$ is described as

$$F_4(s) = \frac{1}{Js + B} \cdot \frac{1}{s} \tag{24}$$

where B is viscous friction coefficient.

The control object of the current regulator $F_3(s)$ is described as

$$G_{i\text{obj}}(s) = \frac{K_v K_m \beta}{(T_{li}s + 1)(T_i s + 1)} \tag{25}$$

where $K_m = 1/R_s$ and $T_{li} = L_q/R_s$. The PI controller of current loop is described as

$$F_3(s) = G_{\mathrm{ACR}}(s) = \frac{K_{pi}(\tau_i s + 1)}{\tau_i s}. \tag{26}$$

Then, the PI controller of speed loop F_2(s) is described as

$$F_2(s) = G_{\mathrm{ASR}}(s) = \frac{K_{pn}(\tau_n s + 1)}{\tau_n s} \tag{27}$$

where K_{pn} and τ_n are the proportional factor and integration time constant of the speed regulator, respectively.

The speed loop is typical II system, it is combined with position loop to obtain a higher order system. In order to analyze the system conveniently, the position regulator F_1(s) is described as

$$F_1(s) = G_{wk}(s) = \frac{K_{pw} K_w}{9.55 s(T_w s + 1)} \tag{28}$$

where K_w is obtained by the reference and actual speed, and T_w is time constant of inertial element. K_{pw} is the proportional factor of the position regulator.

For F_1(s), the input is position reference subtracts position feedback, then adds N_0 disturbances (theta* − theata + N_0) and the output is the speed reference (ω^*). For F_2(s), the input is the speed reference (ω^*) adds N_1 disturbances, and the output is the current reference (i_q^*). For F_3(s), the input is the current reference (i_q^*) adds N_2 disturbances, and the output is the voltage reference (u_q^*). For F_4(s), the input is the voltage reference (u_q^*) adds N_3 disturbances, and the output is the speed reference (ω^*).

To improve the robustness of the servo drive system, the conventional position and speed regulators [F_1(s) and F_2(s)] based on PI is replaced by ISMC, which is expressed in (11) and (15). The optimization processes of ISMC parameters are as follows.

If variables are determined, the Laplace transforms of them can be expressed as

$$\begin{cases} E(s) = \Phi_e(s)R(s) + \sum_{i=0}^{3} \Phi_{eN_i}(s)N_i(s) \\ \Phi_e(s) = 1 - \Phi(s) = \frac{1}{1+F_1(s)F_2(s)F_3(s)F_4(s)} \\ \Phi_{eN_0}(s) = \frac{-F_1(s)F_2(s)F_3(s)F_4(s)}{1+F_1(s)F_2(s)F_3(s)F_4(s)} \\ \Phi_{eN_1}(s) = \frac{-F_2(s)F_3(s)F_4(s)}{1+F_1(s)F_2(s)F_3(s)F_4(s)} \\ \Phi_{eN_2}(s) = \frac{-F_3(s)F_4(s)}{1+F_1(s)F_2(s)F_3(s)F_4(s)} \\ \Phi_{eN_3}(s) = \frac{-F_4(s)}{1+F_1(s)F_2(s)F_3(s)F_4(s)}. \end{cases} \tag{29}$$

According to the objective function and variables of a servo system, k_1, ε_1, c_1, ε_2, and c_2 of ISMC are optimized by the DE algorithm. As shown in Fig. 5, a series of parameters about T_{rise}, $E_{\mathrm{ss\_spe}}$, $\Delta N_{\mathrm{ovdrop}}$, ΔN_{ovup}, T_{rerl}, and T_{renl} are obtained on the basis of speed feedback of the motor rotor, and Y is derived from (23). First, setting initial population $Y = [Y_1, Y_2, \ldots, Y_n]$ and $y_{i,j}$ as the jth component. Then, mutating initial population by (20) the target vector $U_i^{k+1} = [u_{i1}^{k+1}, u_{i2}^{k+1}, \ldots, u_{\mathrm{in}}^{k+1}]$ is calculated, which is generated from mutation vector and source vector by crossing. The DE algorithm can optimize parameters in the next control cycle over and over, and always choose minimum Y from optimization results of each time. Finally, selecting the minimum Y means that suitable parameters k_1, ε_1, c_1, ε_2, and c_2 of ISMC are selected, and control performance reaches given indices. Processes of optimizing k_1, ε_1, c_1, ε_2, and c_2 by DE algorithm are shown in Fig. 7.

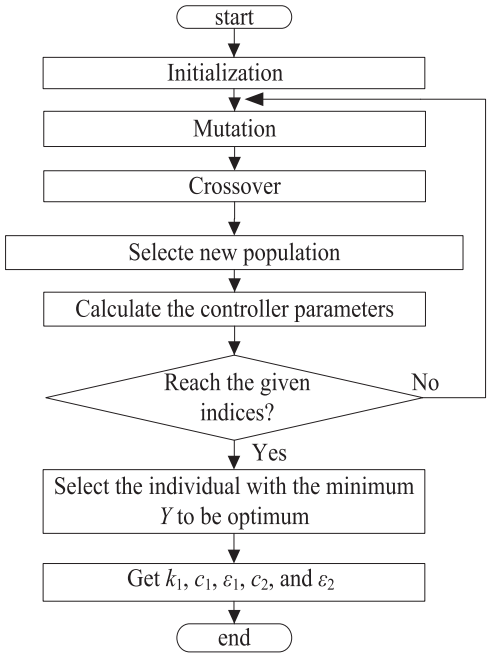

Fig. 7. Main processes of parameters optimization.

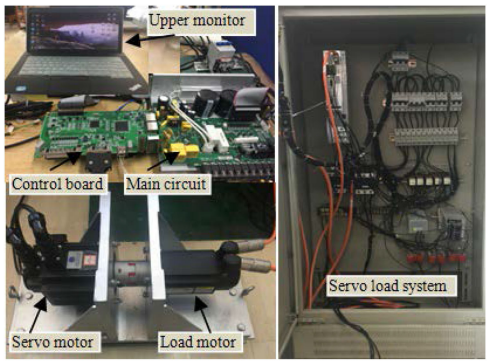

Fig. 8. Experimental platform.

In the processes of optimizing parameters of ISMC by the DE algorithm, the most significant influence factor is iteration. Less value of iteration is unable to make a servo drive system reach given performance indices, larger value of iteration could increase calculation and occupy a lot of DSP memory undoubtedly. Therefore, in order to achieve given performance indices after reaching convergent iteration of the DE algorithm, relative indices of a control system must be given in advance. Then, optimization processes profile of k_1, ε_1, c_1, ε_2, and c_2 are able to be tested, and convergent iteration can be derived as well.

V. Experimental Results

The experimental platform is shown in Fig. 8 and parameters of a servo motor are given in Table I. It is based on the RENESAS DSP SH2A and Lattice FPGA. ISMC algorithm is written by C language in the control board. The feedback

TABLE I
MOTOR PARAMETERS

Symbol	Quantity	Value
P_N	rated power	2 kW
U_N	rated voltage	380 V
n_N	rated speed	2500 rpm
I_N	rated torque	7.7 N·m
f_N	rated frequence	50 Hz
R_s	stator resistance	0.1 Ω
L_d	d-Axis stator inductance	24.3 mH
L_q	q-Axis stator inductance	24.3 m H
J	rotational inertia	0.23 kg·m^2
n_p	number of pole pair	4
ψ	PM flux	0.081 Wb

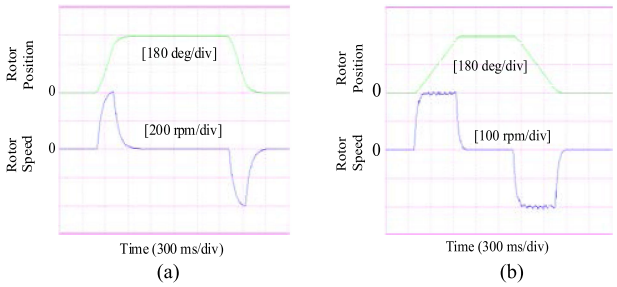

Fig. 9. Responses of position and speed based on individual SMC and ISMC. (a) Individual SMC. (b) ISMC.

information of the servo system is delivered to host computer under the environment of VC ++, and it makes use of Windows application program interface to realize USB interface communication method. DE algorithm is applied to tune parameters offline in the host computer.

A. Correctness Verification of ISMC

The correctness of ISMC is tested with no load in Fig. 9, and sampling rate of ISMC is 62.5 μs. Fig. 9(a) shows that a servo motor switches back and forth between 0° and 180° under individual SMC, which means that position regulator is replaced by the SMC. In this case, the motor rotor speed is uncontrollable and it is more likely to cause high current shock. However, that speed could be controlled by ISMC in Fig. 9(b), and the given $n_{\max}$ is 200 r/min. After the motor rotor speed arrives at 200 r/min, it is limited at 200 r/min. Once actual position of the motor rotor is close to reference position, motor rotor speed is ready to go down until the motor stops. As can be seen, the correctness of ISMC is verified effectively in the servo drive system.

B. Effectiveness Verification of DE-ISMC

The robustness of the proposed method has been mainly investigated under four cases including R_s mismatch, L_d mismatch, low speed crawling, and load disturbance. Before relative performance of ISMC is optimized by DE algorithm, given performance indices should be set. The given performance indices are mentioned in Table II.

TABLE II
PARAMETERS INDICES

Case	Symbol	Quantity	Index
parameter mismatch	T_{rise}	speed rise time (small position)	< 120 ms
parameter mismatch	T_{rise}	speed rise time (middle position)	< 150 ms
parameter mismatch	T_{rise}	speed rise time (large position)	< 250 ms
parameter mismatch	E_{ss_spe}	speed steady error	< 5%
low speed crawling	E_{ss_spe}	speed steady error	< 20%
low speed crawling	T_{rise}	speed rise time	< 100 ms
load disturbance	ΔN_{ovdrop}	speed drop	< 3%
load disturbance	ΔN_{ovup}	speed up	< 3%
load disturbance	T_{rerl}	recovery time of rated load	< 40 ms
load disturbance	T_{renl}	recovery time of no load	< 40 ms

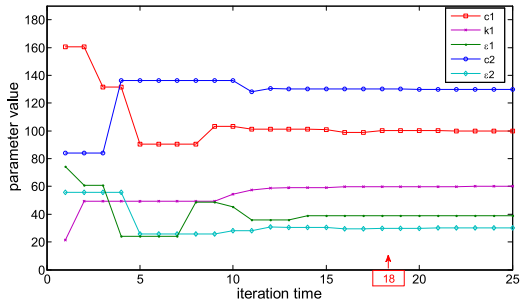

Fig. 10. Optimization processes of five main parameters.

TABLE III
PARAMETERS VALUE

Iteration	$c1$	$k1$	$\varepsilon 1$	$c2$
8th	104	52	50	143
18th	101	63	39	132

The optimization processes of five main parameters k_1, ε_1, c_1, ε_2, and c_2 are shown in Fig. 10. The servo drive system is steady and five parameters are convergent until the 18th iteration, and the system performance reaches given performance indices. For verifying the correctness of convergent iteration and robustness of the system, the system operating values are derived under 8th and 18th with different cases. From experimental results comparisons, it is evident that the servo system performance achieves given indices to enhance robustness of the system after convergent iteration. Initial set of parameters are ready at the beginning of optimization. These parameters, which are chosen according to the empirical value, could guarantee fundamental operation of motor.

The numerical calculation of the five design parameters is shown in Fig. 10. Variable process of ISMC parameters depends on DE algorithm in DSP. Therefore, these five parameters change as optimization iteration changes. For instance, concrete parameters values of 8th and 18th are given in Table III.

1) Verification of Control Performance With R_s Mismatch: Figs. 11–14 illustrate comparative experimental results when the system is under 8th and 18th with R_s mismatch, which aims to the dynamic and steady performance of speed response. In order to realize positioning control with a given speed value of

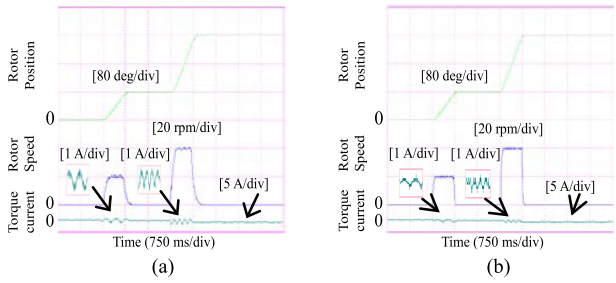

Fig. 11. Comparative results between 8th and 18th under small and middle positions with 2 R_s. (a) 8th. (b) 18th.

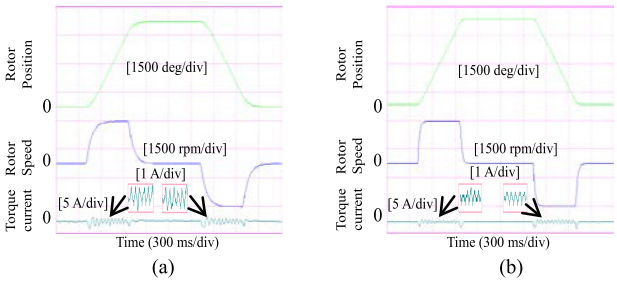

Fig. 12. Comparative results between 8th and 18th under large position with 2 R_s. (a) 8th. (b) 18th.

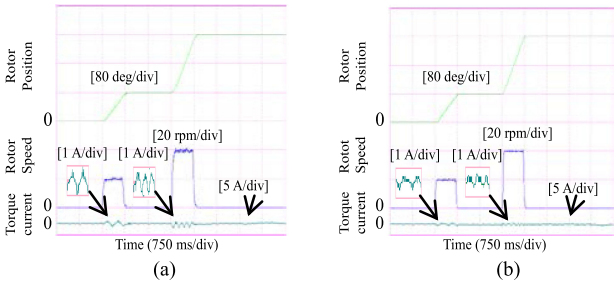

Fig. 13. Comparative results between 8th and 18th under small and middle positions with 0.5 R_s. (a) 8th. (b) 18th.

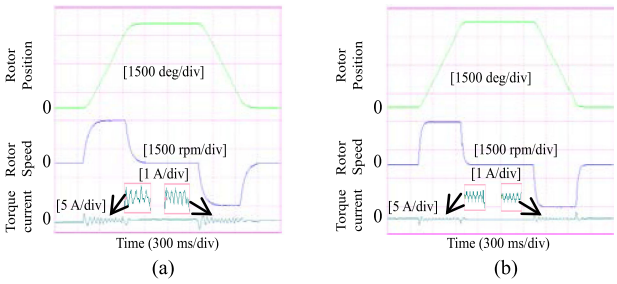

Fig. 14. Comparative results between 8th and 18th under large position with 0.5 R_s. (a) 8th. (b) 18th.

limited maximum speed, which depends on position reference, must be set. The larger the position reference is, the larger the limited maximum speed is. Fig. 11 shows position response, trapezoidal speed profile and torque current under small and middle positions of the system with 2 R_s mismatch. Fig. 12 shows analogous comparative results under large position with 2 R_s mismatch. Similarly, Figs. 13 and 14 also verify analogous comparative results with 0.5 R_s mismatch. It is clear that rise

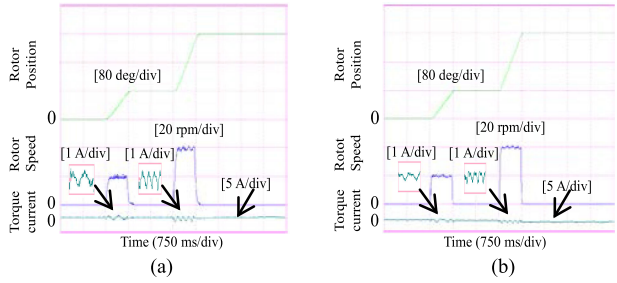

Fig. 15. Comparative results between 8th and 18th under small and middle positions with 2 L_d. (a) 8th. (b) 18th.

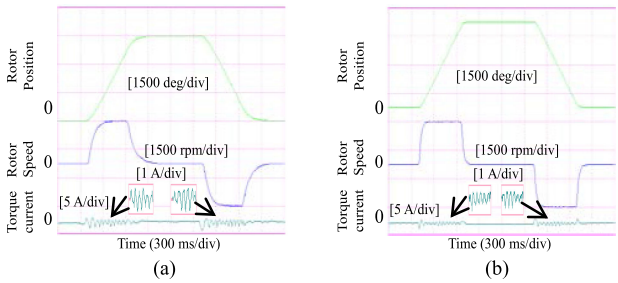

Fig. 16. Comparative results between 8th and 18th under large position with 2 L_d. (a) 8th. (b) 18th.

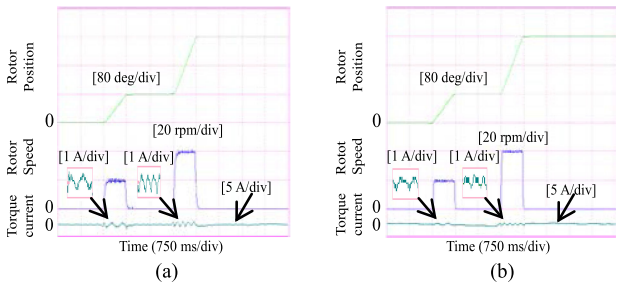

Fig. 17. Comparative results between 8th and 18th under small and middle positions with 0.5 L_d. (a) 8th. (b) 18th.

time and steady error of motor speed under 18th are smaller than that under 8th, and vibration of torque current is smaller under 18th. Meanwhile, speed response reaches given performance indices until 18th. The conclusion is drawn that the effectiveness of ISMC is verified with R_s mismatch.

2) Verification of Control Performance With L_d Mismatch: Similarly, Figs. 15–18 illustrate comparative experimental results when the system is under 8th and 18th with L_d mismatch. When the *d*-axis inductance is under 2 L_d or 0.5 L_d, alike experiments are verified. Fig. 15 shows position response, trapezoidal speed profile, and torque current under small and middle positions of the system with 2 L_d mismatch. Fig. 16 shows analogous comparative results under large position with 2 L_d mismatch. Figs. 17 and 18 also verify analogous comparative results with 0.5 L_d mismatch. The conclusion is drawn that steady state error of speed and vibration of torque current decrease obviously. In addition, speed response is faster under 18th and relative performance reaches to given performance indices until 18th.

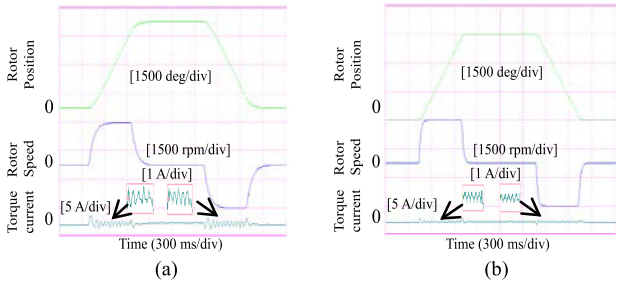

Fig. 18. Comparative results between 8th and 18th under large position with 0.5 L_d. (a) 8th. (b) 18th.

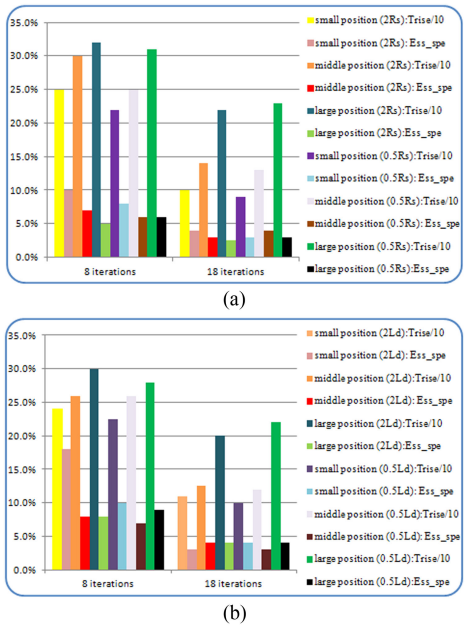

Fig. 19. Histogram of the comparative results between 8th and 18th with parameter mismatch. (a) R_s mismatch. (b) L_d mismatch.

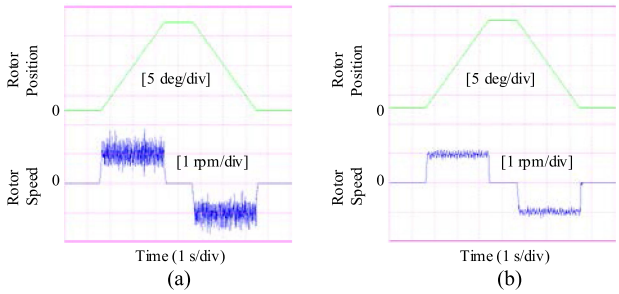

Fig. 20. Comparative results between 8th and 18th with low speed crawling. (a) 8th. (b) 18th.

In order to show the experimental data of control performance more clearly under 8th and 18th with parameter mismatch, the histogram of the comparative results is given in Fig. 19.

3) Verification of Control Performance With Low Speed Crawling: The low speed crawling is a common phenomenon in a servo drive system, and it could cause vibration very often. Comparative results of control performance are under 8th and 18th. Reference position switches between 0° and 15° at ±1 r/min in Fig. 20. It is obvious that motor rotor is

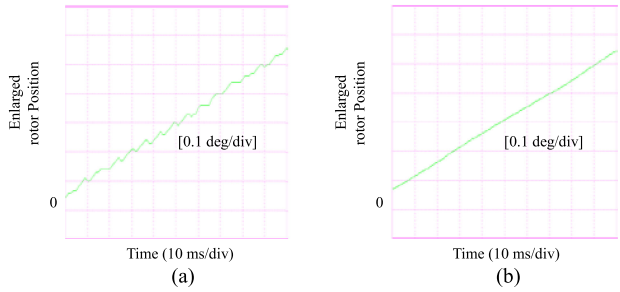

Fig. 21. Position enlarged figures between 8th and 18th with low speed crawling. (a) 8th. (b) 18th.

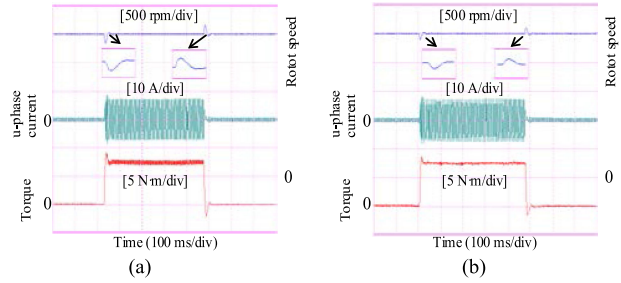

Fig. 22. Comparative results between 8th and 18th with load disturbance at 2500 r/min. (a) 8th. (b) 18th.

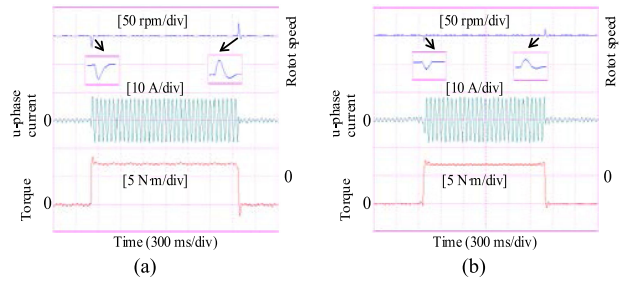

Fig. 23. Comparative results between 8th and 18th with load disturbance at 250 r/min. (a) 8th. (b) 18th.

fluctuating at ±1 r/min, and fluctuation of speed response is about 0.5 r/min under 8th ($E_{\mathrm{ss\_spe}} = 50\%$, $T_{\mathrm{rise}} = 120$ ms) in Fig. 20(a), but speed response is optimized and fluctuation is about 0.1 r/min under 18th ($E_{\mathrm{ss\_spe}} = 10\%$, $T_{\mathrm{rise}} = 80$ ms) in Fig. 20(b). Position response is enlarged at +1 r/min under 8th and 18th in Fig. 21. Comparing Fig. 21(a) and (b), position response rises more smoothly under 18th, and fluctuation of speed response decreases obviously. It is validated that control performance of low speed reaches to control indices under 18th, and relieves low speed crawling phenomenon effectively. The conclusion is drawn that relative performance of low speed crawling reaches to given performance indices until 18th.

4) Verification of Control Performance With Load Disturbance: Figs. 22 and 23 show comparative experimental results under 8th and 18th, respectively. The load steps up from no load to the rated load, and steps down from the rated load to no load. Speed reference is 2500 r/min in Fig. 22 and 250 r/min in Fig. 23. Dynamic performance of step load steps up and down is enlarged. It is shown that better robustness and more rapid dynamic response are obtained under 18th when the load torque

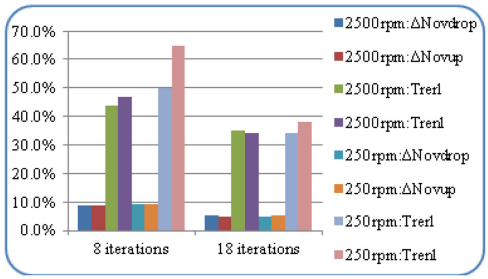

Fig. 24. Histogram of the comparative results between 8th and 18th with load disturbance.

varies suddenly. The conclusion is drawn that the relative performance reaches control indices until 18th, and DE-ISMC plays a role of "anti-disturbance."

In order to show the difference of control performance more clearly under 8th and 18th with load disturbance, the histogram of the comparative results is given in Fig. 24.

VI. Conclusion

A novel DE-ISMC method is proposed to guarantee that a motor rotor can arrive at given position with given travel speed in a servo drive system. The travel speed means the speed in speed control region $\omega = \omega_{\max}$. In order to make system performance achieve given indices, indirectly the robustness of system is improved as well. After suitable iteration of DE algorithm, main parameters of ISMC are optimized well. It is more efficient to achieve dynamic and steady given performance indices of position and speed response within limited iterations by using DE algorithm. In addition, DE-ISMC reduces the low speed crawling phenomenon effectively under convergent iteration. In other words, DE-ISMC is feasible to improve robustness and achieve given control indices of a servo system after a suitable iteration.

Acknowledgment

C. Du especially appreciates the powerful spirit support from his mother, his father, and his fiancée, K. Lu.

References

[1] J. Ye, B. Bilgin, and A. Emadi, "An extended-speed low-ripple torque control of switched reluctance motor drives," *IEEE Trans. Power Electron.*, vol. 30, no. 3, pp. 194–202, Mar. 2015.

[2] Z. Li, J. Chen, G. Zhang, and M. Gan, "Adaptive robust control of servo mechanisms with compensation for nonlinearly parameterized dynamic friction," *IEEE Trans. Control Syst. Technol.*, vol. 21, no. 1, pp. 194–202, Jan. 2013.

[3] L. Juarez, "Robust trajectory tracking of a delta robot through adaptive active disturbance rejection control," *IEEE Trans. Control Syst. Technol.*, vol. 23, no. 4, pp. 1387–1398, Jul. 2015.

[4] H. W. Chow and N. C. Cheung, "Disturbance and response time improvement of submicrometer precision linear motion system by using modified disturbance compensator and internal model reference control," *IEEE Trans. Ind. Electron.*, vol. 60, no. 1, pp. 139–150, Jan. 2013.

[5] Z. Qiu, M. Jankovic, J. Sun, and M. Santillo, "Composite adaptive internal model control and its application to boost pressure control of a turbocharged gasoline engine," *IEEE Trans. Control Syst. Technol.*, vol. 23, no. 6, pp. 2306–2315, Nov. 2015.

[6] J. W. Jung, V. Q. Leu, T. D. Do, E.-K. Kim, and H. H. Choi, "Adaptive PID speed control design for permanent magnet synchronous motor drives," *IEEE Trans. Power. Electron.*, vol. 30, no. 2, pp. 900–908, Feb. 2015.

[7] A. Saghafinia, H. W. Ping, M. N. Uddin, and K. S. Gaeid, "Adaptive fuzzy sliding-mode control into chattering-free IM drive," *IEEE Trans. Ind. Appl.*, vol. 51, no. 1, pp. 692–701, Jan. 2015.

[8] S. Li, M. M. Zhou, and X. H. Yu, "Design and implementation of terminal sliding mode control method for PMSM speed regulation system," *IEEE Trans. Ind. Inform.*, vol. 9, no. 4, pp. 1879–1891, Nov. 2013.

[9] M. T. Angulo and R. V. Carrillo-Serrano, "Estimating rotor parameters in induction motors using high-order sliding mode algorithms," *IET Control Theory Appl.*, vol. 9, no. 4, pp. 573–578, Feb. 2015.

[10] Y. Fan, L. Zhang, M. Cheng, and K. T. Chau, "Sensorless SVPWM-FADTC of a new flux-modulated permanent-magnet wheel motor based on a wide-speed sliding mode observer," *IEEE Trans. Ind. Electron.*, vol. 62, no. 5, pp. 3143–3151, May 2015.

[11] X. Zhang, L. Sun, K. Zhao, and L. Sun, "Nonlinear speed control for PMSM system using sliding-mode control and disturbance compensation techniques," *IEEE Trans. Power Electron.*, vol. 28, no. 3, pp. 1358–1365, Mar. 2013.

[12] X. Zhang and G. H. B. Foo, "A robust field-weakening algorithm based on duty ratio regulation for direct torque controlled synchronous reluctance motor," *IEEE Trans. Mechatron.*, vol. 21, no. 2, pp. 765–773, Apr. 2016.

[13] J. F. Pan, S. W. Or, Y. Zou, and N. C. Cheung, "Sliding-mode position control of medium-stroke voice coil motor based on system identification observer," *IET Elect. Power Appl.*, vol. 9, no. 9, pp. 620–627, Nov. 2015.

[14] J. Ye, P. Malysz, and A. Emadi, "A fixed-switching-frequency integral sliding mode current controller for switched reluctance motor drives," *IEEE Trans. Power Electron.*, vol. 3, no. 2, pp. 381–394, Jun. 2015.

[15] M.-Y. Chen and J.-S. Lu, "High-Precision motion control for a linear permanent magnet iron core synchronous motor drive in position platform," *IEEE Trans. Ind. Inform.*, vol. 10, no. 1, pp. 99–108, Feb. 2014.

[16] S. Lin, Y. Cai, B. Yang, and W. D. Zhang, "Electrical line-shafting control for motor speed synchronisation using sliding mode controller and disturbance observer," *IET Control Theory Appl.*, vol. 11 no. 2, pp. 205–212, 2017.

[17] C. S. Ting, Y. N. Chang, B. W. Shi, and J. F. Lieu, "Adaptive backstepping control for permanent magnet linear synchronous motor servo drive," *IET Elect. Power Appl.*, vol. 9, no. 3, pp. 265–279, 2015.

[18] H. Y. Zhu, C. K. Pang, and T. J. Teo, "Integrated servo-mechanical design of a fine stage for a coarse/fine dual-stage positioning system," *IEEE Trans. Mechatron.*, vol. 21, no. 1, pp. 329–338, Feb. 2016.

[19] Y. Z. Zhou, W. C. Yi, L. Gao, and X. Y. Li, "Adaptive differential evolution with sorting crossover rate for continuous optimization problems," *IEEE. Trans. Cybern.*, vol. 47, no. 9, pp. 2742–2753, Sep. 2017.

[20] Y. Mao, S. Niu, and Y. Yang, "Differential evolution-based multiobjective optimization of the electrical continuously variable transmission system," *IEEE. Trans. Ind. Electron.*, vol. 65, no. 3, pp. 2080–2089, Mar. 2018.

[21] Y. P. Shen and Y. N. Wang, "Operating point optimization of auxiliary power unit using adaptive multi-objective differential evolution algorithm," *IEEE Trans. Ind. Electron.*, vol. 64, no. 1, pp. 115–125, Jan. 2017.

[22] X. Y. Xu and H. Lin, "Integrated design for permanent magnet synchronous motor servo systems based on dynamic sliding mode control," *Trans. China Electrotechnical Soc.*, vol. 29, no. 5, pp. 77–83, May 2014.

Zhonggang Yin (M'13) was born in Shandong, China, in 1982. He received the B.S., M.S., and Ph.D. degrees in electrical engineering from the Xi'an University of Technology, Xi'an, China, in 2003, 2006, and 2009, respectively.

In 2009, he joined the Department of Electrical Engineering, Xi'an University of Technology, where he is currently a Professor. His research interests include high-performance control of AC motors and digital control of power converters.

Lei Gong was born in Shaanxi, China, in 1993. He received the B.S. and M.S. degrees in electrical engineering from the Xi'an University of Technology, Xi'an, China, in 2015 and 2018, respectively.

His research interests include high-performance control of servo motors and the optimization of their efficiency and parameters.

Chao Du (S'17) was born in Shaanxi, China, in 1991. He received the B.S. and M.S. degrees in electrical engineering from the Xi'an University of Technology, Xi'an, China, in 2013 and 2016, respectively. He is currently working toward the Ph.D. degree in electrical engineering at the Xi'an University of Technology. His research interests include high-performance AC drive systems and the optimization of their efficiency and parameters.

Jing Liu was born in Anhui, China, in 1982. She received the B.S., M.S., and Ph.D. degrees in electronic engineering from the Xi'an University of Technology, Xi'an, China, in 2003, 2006, and 2009, respectively.

In 2009, she joined the Department of Electronic Engineering, Xi'an University of Technology, where she is currently an Associate Professor. Her research interests include power semiconductor devices and their application to power electronic devices.

Yanru Zhong was born in Xi'an, China, in 1950. He received the B.S. degree in electrical engineering from the Xi'an Jiaotong University, Xi'an, China, in 1975 and the M.S. degree in electrical engineering from the Xi'an University of Technology, Xi'an, China, in 1983.

He was with the Xi'an University of Technology in 1983. He was a Visiting Scholar with the Department of Electrical Engineering, Sophia University, Tokyo, Japan, in 1987. Since 1993, he has been a Professor with Xi'an University of Technology. His research interest includes power electronics, particularly inverters and AC drive systems.